ADVANCED PROPULSION COLLISION DAMAGE DUE TO UNMANNED AERIAL SYSTEM INGESTION

Yangkun Song[1], Kevin Schroeder[2], Brandon Horton[3], and Javid Bayandor[4]
[1, 2, 3]Crashworthiness for Aerospace Structure and Hybrids (*CRASH*) Lab
Virginia Tech, Blacksburg, VA, 24061
Email : bayandor@vt.edu

Abstract

An explicit numerical analysis was employed to assess the dynamic damage development in advanced high-bypass propulsion system in the event of a drone ingestion. CFRP was implemented in the fan blade design and rate-dependent metal alloy properties were considered. Details of damage history on the subjected propulsion system were discussed.

1 Introduction and Motivation

Unmanned aerial systems (UAS) have had a huge increase in popularity in the last few years. They are cheap, lightweight, and extremely versatile. There applications range from agriculture to security. Studies have shown that the UAS market is expected to grow to 2.5 billion dollars by 2025 [1].

Recently, the FAA approved the use of UAS in commercial applications in June 2016 [2]. This implies that air traffic getting more complicated by UAS. As popular as UAS are in the commercial market, they are currently more available in the private and hobbyist market.

In the private market, there is an amount of ambiguity, as the owners do not need to be licensed or register their vehicle. The hobby used may not be award of all the potential risk and the required restrictions associated with flying their UAS. Additionally there is little accountability for the hobbyist flyer as drones cannot readily be tracked or identified. This presents a significant danger to the established aviation industry.

Gettinger and Michel collected and analyzed all the reported drone sightings around manned aircraft in the USA. Their study spanned a year and a half and comprised of 921 incidents. 58.8 % of those incident were within a 5-mi radius of an airport and 90.2 % were sighted above 400 ft. Both of which are restricted for UAS to fly in [3].

Currently, the FAA has numerous regulations for soft body impact and ingestions [4-6]. It is believed that an encounter with a soft body ingestion will cause less damage than an UAS impact or ingestion of similar size and mass due to the material strength of the internal components such as the batteries, motors, the frame, cameras and additional payloads. These hard body ingestions are not yet understood and no certification is yet required for such an event.

In a hearing before the U.S. Subcommittee on Aviation it was exposed that a large conflict in placing regulations on UAS pilots is the lack of data available. Rep. Todd Rokita tried to draw the comparison between a Canadian goose collision and UAS collision. It is known that UAS are comprised of heavier and stiffer components than that of

birds, but it was concluded that at the current time the comparison was unquantifiable [7]. In this paper a UAS of similar size and mass of a typical adult Canadian goose will be modeled and ingested into a modern high bypass engine. While this study does not draw a direct comparison between a UAS and goose ingestion scenario, it does aims to further the understanding of hard body ingestions, in an effort to begin to quantify the risk presented by the increase in UAS.

2 Computational Setup

The current UAS market has a significant diversity between its numerous types of drones. These drones can be fixed winged or multirotor. Additionally the size, mass, and number of motor can vary from drone to drone. For this analysis it was desired to model a UAS that has the capability to easily exceed the exceed the 400 ft UAS ceiling as well as be large enough to be a reasonable threat to a high bypass propulsion system in the event of an ingestion. The drone model that was developed for the investigation was 5.4 kg in mass and a maximum diameter of 1.0 m.

The model contains the primary components of the UAS. The frame, motors, batteries, payload, and gimbal are all included in the model. Since a high fidelity multicopter UAS would be prohibitively complex to simulate comprehensive damage response prediction, the primary components were simplified and geometrically defeatured to reduce computational expense. The motor, battery, payload, and gimbal each used a bilinear constitutive damage material models reflecting their respective primary material. The UAS frame, including the arms, were modeled with a full composite material model utilizing Chang matrix failure criterion [8]. Components that offer little mechanical strength, such as rotor blades, electronics, and wires are considered to be insignificant in the ingestion scenario and are not explicitly modeled, although their mass is distributed in the model to insure that the mass distribution is representative of an actual UAS.

For this analysis it was desired to find a commercially available UAS with roughly the same dimensions as that of a typical Canadian goose. According to the national geographic, a typical Canadian geese is between 3 and 9 kg and has a typical body size 0.76-1.10 m [9]. Figure 1 depicts and labels the major UAS component in the model, while table 1 records the mass of each component.
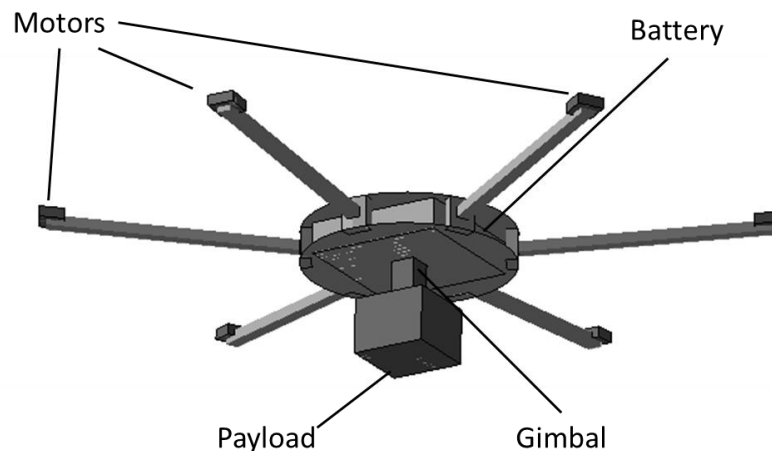
Fig. 1 Developed UAS model for ingestion

Table 1 UAS bill of materials

	Motors	Frame	Battery	Payload	Gimbal	Total
Mass (kg)	0.95	1.45	1.9	0.9	0.2	5.4
Qty.	6	1	1	1	1	-
Material	Copper	CFRP	Li-ion	Surrogate	Aluminum	-

Table 2 Material properties solid components

Component	Material	Denisty kg/m3	Modulus (GPa)	Poisson Ratio -	Yield Stregth (MPa)	Tangent Modulus (MPa)
Battery	Li-Po	1135	0.5	0.3	30.0	50.0
Motor	Copper	7700	117.0	0.34	70.0	300.0
Gimbal	Aluminum	2700	68.9	0.33	276.0	27.6
Payload	Surrogate	1000	50.0	0.3	500.0	50.0

The virtual propulsion system used in this study is a 2.9 m diameter high-bypass commercial jet engine. In order to achieve a high fidelity damage prediction, the virtual propulsion model includes fully assembled front inlet fan section, low pressure compressor (LPC), casings, and bearing and shaft system. Considering the contemporary fan blade design, the advanced aerodynamic carbon fiber fan blade was implemented. The orientation of each individual orthotropic ply was assigned based on a reduced thickness fan blade developed by Miller et. al [10,11]. The propulsion system used in the analysis can be seen in fig. 2. The virtual system used in this investigation was developed previously and successfully predicted the dynamic response and the damage mechanics of the system subjected to a foreign object ingestion [12-14]. By employing the same virtual engine model, a drone ingestion into a propulsion system simulation was conducted.

The chance to encounter UAS for the airplane becomes higher when the airplane flies at low altitude such as taking off or landing. Therefore, the ingestion scenario was assumed when a propulsion system is being operated at max thrust during taking off. The operating condition varies among each engine designs. For the virtual propulsion, the rotational speed of the entire fan assembly is set as 2160 RPM (226 rad/s) [15, 16]. Considering the stall speed for a jumbo passenger aircraft during taking off, the drone ingestion speed was defined as 92 m/s.
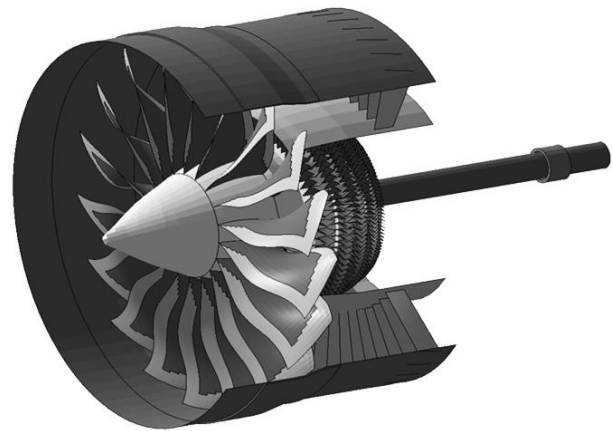
Fig. 2 Virtual Propulsion System

3 Results and Discussion

Upon ingestion, the UAS impacts 7 of the 18 blades. Each of the affected blades are subjected to various amounts of damage

depending on what part of the UAS made contact with them. Blades that were only impacted by one or two of the UAS arms experienced little to no permanent damage, while the blades that impacted the more UAS arms as well their attached motors began to see notable irreversible damage, typically on the blades leading edge. As expected, blades that contacted the UAS hub, where the most substantial components are located (i.e. the battery, payload, and gimbal) saw the most severe damage. These blades were subjected to peak forces up to 82.2 kN in a 0.0125 sec impact window.
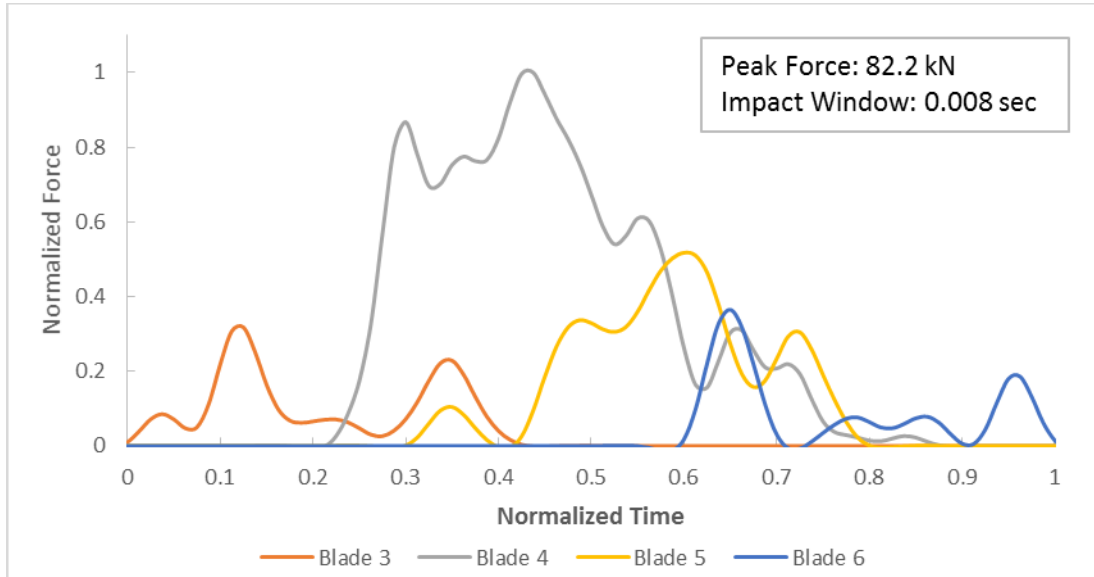
Fig. 3 Force-time history of blades 3-6

Table 3 Tabularized blade impact sequence

	Blade 1	Blade 2	Blade 3	Blade 4	Blade 5	Blade 6	Blade 7
Arm	1	2	3	-	2	3	-
Motor	-	1	1	-	-	1	2
Frame	-	-	-	1	1	-	-
Battery	-	-	-	1	1	-	-
Payload	-	-	-	1	1	-	-
Gimbal	-	-	-	1	-	-	-

Figure 3 shows the force time history of the impacted fan blades excluding less significantly impacted blades 1, 2, and 7 who only contact two or less UAS arms (the impact window of Blades 3-6 was 0.0045 seconds less than the full impact window).

Table 3 summarizes the impact sequence of each fan blade by tabularizing which blades were impacted by various components of the UAS. Blade 3 was the last blade to not slice through the main hub of the UAS frame.
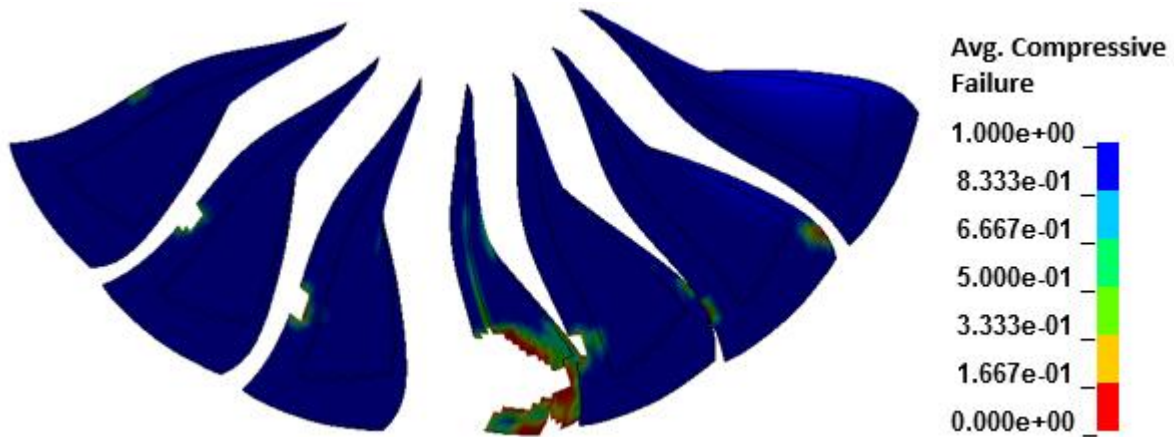
Fig. 4 Post-impact average composite damage fringe plot

The following blade sliced into the center of the UAS hub. Hence, the total impulse on blade 4 is significantly larger than any other fan blades subjected to impact and subsequently it experienced the heaviest damage of any of the other blades. This instantly resulted in partial removal of Blade 4.

5. Figure 4 shows the composite damage of the the subjected fan blades after the UAS fully passed through the front inlet section. Figure 4 depicts the average compressive damage through the thickness of each blade, where 1 is no damage at all and 0 is fully damaged.
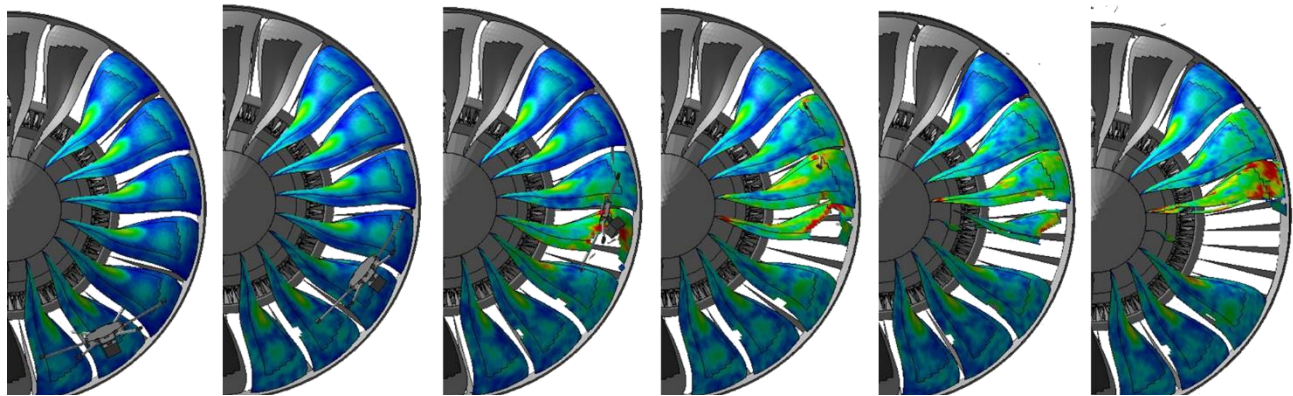
Fig. 5 Full time lapse of ingestion scenario

After the major interaction, the force magnitude of the neighboring fan blades gradually reduced. Blade 5 was subjected to the second largest impulse not because of its slice pattern on the UAS but because it was exposed to the large debris created from the blade 4 impact, included the ejected pieces of fan blade. Blade 6 experience the same order of magnitude of Blade 3 because it was shielded from the remaining debris by Blade

The post-impact damage magnitude continuously elevated in a combination of continuous rotation and casing contact. As a result, an extremely high bending load developed at the fourth fan blade root. The dmaage surpassed the untilmate strength and the fan blade was ejected from the fan assembly. After the ejection, the ejecta was then lodged in between the adjacent fan blade

and casing. This resulted in critical damage on the adjacent fan blade.

The detachment of the fan blade directely resulted in an imbalanced rotation of the entire fan assembly. This will esclate the damage on the entire propulsion system, since the clearance between the fan blades and casing are a fraction of centimeter. Based on previous work [14], remain debris from the fan blade out can be ingested by the LPC resulting in compressor stall.

4 Conclusion

Base on the preceding analysis, the ingestion of a 5.6 kg UAS potentially cause catastrophic damage to the engine and poses a significant threat to the airliner, its crew, cargo, and passengers throughout the preliminary investigation. To the author's knowledge, this study is the first attempt to quantify the dynamic response and the detailed damage mechanics of a UAS ingestion into a high-bypass commercial jet engine scenario. Due to the complicated nature of ingestion scenario, each case will unique. Though, the work presented in this paper represents a single ingestion example of such an event. Further investigation should be performed to classify key aspects of the ingested drone and quantifying the threshold size and mass of UAS that can cause catastrophic failure to commercial turbofans.

Reference

[1] Jenkins, D., and Vasigh, B., "The economic impact of unmanned aircraft systems integration in the United States," 2013, pp. 1–40.

[2] FAA, "Operation and Certification of Small Unmanned Aircraft Systems; Final Rule" June 2016

[3] Gettinger, D., Michel, A. H., and Holland Michel, A., "Drone sightings and close encounters: An analysis," *Bard College Center for the Study of the Drone*, 2015, p. 28.

[4] FAA, "Federal Aviation Regulations/Aeronautical Information Manual (FAR/AIM) 33.77: Rain and hail ingestion certification standards, A.C. No. 33.77," 2014.

[5] FAA, "Federal Aviation Regulations/Aeronautical Information Manual (FAR/AIM) 2015: Bird ingestion certification standards, A.C. No. 33.76," 2009.

[6] FAA, "Turbine engine rotor blade containment/durability (AC No. 33.94)," 1990.

[7] *"Ensuring Aviation Safety in the Era of Unmanned Aircraft Systems: Hearings before the Subcommittee on Aviation (2015)"* (statement of Chairman Frank LoBiondo)

[8] Chang, F.-K., and Chang, K.-Y., "A progressive damage model for laminated composites containing stress concentrations," *Journal of composite materials*, vol. 21, 1987, pp. 834–855.

[9] "*Canada Geese, Canada Goose Pictures, Canada Goose Facts.*" National Geographic. National Geographic Society, Accessed 17 July 2016.

[10] Miller, S. G., Handschuh, K., Sinnott, M. J., Kohlman, L. W., Roberts, G. D., Martin, R. E., Ruggeri, C. R., and Pereira, J. M., "Materials, Manufacturing, and Test Development of a Composite Fan Blade Leading Edge Subcomponent for Improved Impact Resistance," 2015.

[11] Hexcel Corporation, "HexPly 8551-7 Epoxy Matrix," 2006, pp. 1–4.

[12] Song, Y., and Bayandor, J., "Comprehensive soft impact damage methodology for advanced high bypass ratio turbofan engines," *ASME 2014 4th Joint US-European Fluids Engineering Division Summer Meeting collocated with the ASME 2014 12th International Conference on Nanochannels, Microchannels, and Minichannels*, American Society of Mechanical Engineers, 2014, pp. V01BT13A004–V01BT13A004.

[14] Song, Y., and Bayandor, J., "Novel Implementation of Fluid-Solid Interaction Analysis in Air Breathing Propulsion Systems," *ASME/JSME/KSME 2015 Joint Fluids Engineering Conference*, American Society of Mechanical Engineers, 2015, pp. V001T13A001–V001T13A001.

[15] Song, Y., and Bayandor, J., "Analysis of Progressive Dynamic Damage Caused by Large Hailstone Ingestion into Modern High Bypass Turbofan Engine."

[16] FAA, "Type Certificate Data Sheet (E00078NE)," 2008.

[17] EASA, "European Aviation Safety Agency EASA TYPE CERTIFICATE DATA SHEET," 2013, pp. 1–9.

Copyright Statement